A NON-RECIPROCAL LAMB-WAVE DELAY LINE EXPLOITING ACOUSTOELECTRIC EFFECT IN SINGLE CRYSTAL GERMANIUM

Faysal Hakim, Mehrdad Ramezani, Sushant Rassay, and Roozbeh Tabrizian
Department of Electrical and Computer Engineering, University of Florida, Gainesville, USA

ABSTRACT

The paper reports on the use of acoustoelectric amplification in single crystal germanium (Ge) to achieve non-reciprocity in radio frequency (RF) delay lines operating based on Lamb waves. Such delay lines are important in attaining integrated full-duplex wireless communication systems, an integral part of forthcoming 5G applications. Fundamental anti-symmetric (A_0) and symmetric (S_0) Lamb waves are excited in Ge waveguide using a 200nm-thik aluminum nitride (AlN) piezoelectric transducer with unidirectional IDTs. The generated traveling waves are then amplified through deformation potential coupling between the wave and DC accelerated electrons in Ge. Finite element model (FEM) is used to identify A_0 and S_0 modes at 72 MHz and 267 MHz respectively. Analytical models, based on acoustoelectric interaction in single crystal Ge, is used to predict strong amplification of 18 dB/mm (A_0) and 26 dB/mm (S_0). Fabricated delay lines operating at 70 MHz (A_0) and 226 MHz (S_0) demonstrate forward transmission amplification of ~6 dB and ~7 dB upon application of 35 V and 45 V, respectively. In particular, a non-reciprocal transmission ratio of 20 dB is measured for the S_0 mode, showcasing the prospects of Ge-based RF delay lines in realization of full-duplex front-end modules.

KEYWORDS

Lamb waves, acoustoelectric amplification, germanium, deformation potential coupling, non-reciprocal.

INTRODUCTION

The forthcoming wireless protocols (i.e. 5G and beyond) targets the use of full-duplex scheme to enhance spectrum use efficiency and data communication rate, larger bandwidth and lower latency. In this regard, integrated non-reciprocal spectral processors, which allows simultaneous data transmission and reception at the same band, have drawn much attention in applied physics and engineering disciplines recently. Non-reciprocal spectral processors have been previously demonstrated mostly in macro scale such as ferrite-based circulators and isolators. Recently, a new wave of integrated non-reciprocal technologies are demonstrated through utilization of operating based on time-variant architectures [1,2], asymmetric physical non-linearities [3] and directional polarization in electromechanical transducers [4-6]. Among these, DC polarized acoustic waveguide allows extreme frequency scaling over 0.3-30 GHz as well as offering large dynamic range of operation and low insertion loss. Non-reciprocity in DC polarized acoustic waveguide originates from the acoustoelectric (AE) amplification that occurs when propagating wave interacts with drifting electrons in piezoelectric semiconductors. The interaction results in amplification of propagating waves if drift velocity of electrons is greater than the travelling wave velocity [7]. The interaction and thus the energy/momentum transfer from electrical domain to acoustic domain depends largely on (1) piezoelectric coupling, responsible for generation of the travelling electric field along with the acoustic wave, and (2) electron mobility, which defines the drift velocity of electrons. Earlier demonstrations of the acoustoelectric amplification, in semiconductor piezoelectric materials such as gallium nitride, were only providing limited non-reciprocal transmission ratio (NTR) as most of piezoelectric semiconductors lack one or both abovementioned properties. Recent demonstrations of large NTR values have been relying on wafer level bonding of non-piezoelectric semiconductors on piezoelectric lithium niobite. These solutions mainly suffer from wafer bonding challenges and do not offer true CMOS integrability.

In this paper, we demonstrate an integrated non-reciprocal delay-line using acoustoelectric amplification in AlN-on-Ge waveguides (Figure 1(a)). Through deformation potential coupling in electronic band structure of single crystal Ge, additional lattice strain induced by DC accelerated electrons results in wave amplification. Benefiting from large deformation potential constant and electron mobility, substantial acoustoelectric amplification has been observed at lower DC biases in Ge waveguides compared to that of literature. Our analytical and numerical models, along with fabricated delay lines highlight the potential of single crystal Ge in realizing CMOS compatible non-reciprocal device in chip scale for emerging 5G processors.

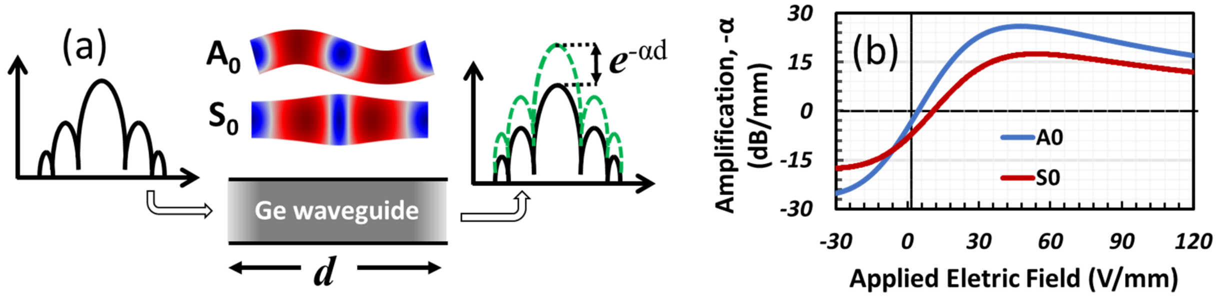

Figure 1: (a) Spectral representation of acoustoelectric amplification (<0) along with displacement profiles of anti-symmetric (A_0) and symmetric (S_0) lamb wave modes in Germanium (Ge) (b) Estimation of acoustoelectric amplification in Ge at different applied electric fields for A_0 and S_0 lamb wave modes having phase velocity of 1790 m/s and 4215 m/s.

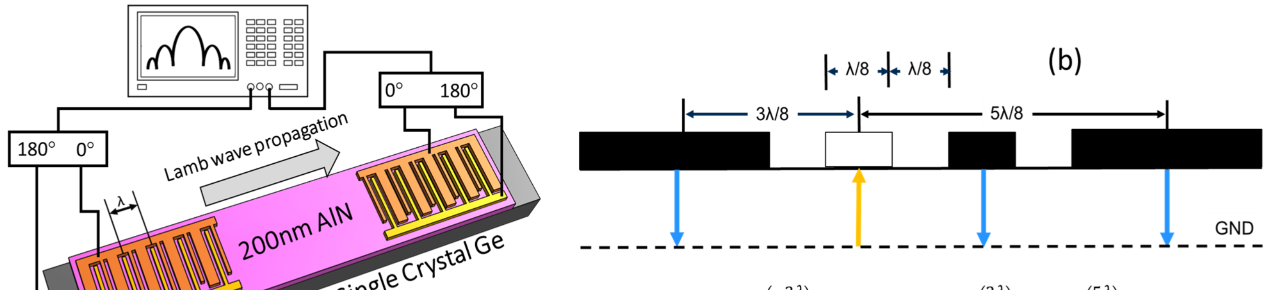

$$H_{\mathrm{IDT}}(f) = -e^{-j\beta\left(-\frac{3\lambda}{8}\right)} + e^{-j\beta(0)} - e^{-j\beta\left(\frac{2\lambda}{8}\right)} - e^{-j\beta\left(\frac{5\lambda}{8}\right)} = 2\angle 90°$$

Figure 2: (a) Schematic demonstration of the AlN-on-Ge delay line and measurement setup for obtaining frequency response. The delay line comprises of two set of single-phase unidirectional transducers (SPUDT). The input and output SPUDTs are connected to Vector Network Analyzer (VNA) through a RF Balun for out of phase voltage actuation and sensing respectively. (b) Electric field distribution inside piezoelectric layer upon application of out of phase voltages in single phase unidirectional transducers (SPUDT) using RF Balun. The blue and yellow arrows represent the direction of electric fields when 0° and 180° phase shifted voltages are applied in corresponding electrodes. The dashed line at the bottom indicates grounded electrode. Fourier analysis of SPUDTs show that the generated wave has phase angle of 90° which interferes constructively with reflectors situated at 5 /8 and destructively with reflectors situated at 3 /8 which validates the unidirectional nature of the SPUDTs.

GAIN-LOSS MECHANISM IN GE

The multi-valley configuration of conduction band in Ge makes phonon-electron interaction favorable through deformation potential coupling. Conceptually, a mechanical wave propagating through a Ge waveguide redistributes free charge carriers in electronic band structure along its propagating path via inter-valley scattering mechanism. The anharmonicity of free carrier relaxation with acoustic wave propagation results in uneven bunching of electrons behind or ahead of acoustic wave, which results in acoustoelectric attenuation or amplification, respectively. The attenuation parameter (α) can be estimated as [7]:

$$\alpha = \frac{n_c \Xi_u^2}{9 v_s^3 k_B T \rho} \frac{\omega^2 \tau_R \left(1 - \frac{v_d}{v_s}\right)}{\left[1 + \left(1 - \frac{v_d}{v_s}\right)^2 \omega^2 \tau_R^2\right]} \qquad (1),$$

where, n_c = density of electrons, Ξ_u = deformation potential constant, τ_R= intervalley relaxation time, v_s = acoustic velocity, v_d = electron drift velocity and other symbols have their usual meanings. Understandably, attenuation will become negative (i.e amplification in Figure 1(a)) when $v_d > v_s$ in Eq.(1). This can be achieved by applying a strong DC electric field (E_{dc}) across Ge waveguide which will launch electron 'faster' than the travelling acoustic wave. Owing to high electron mobility (μ_n = 3900 cm^2/V.s) and slow acoustic velocity (v_d = 2000 – 5000 m/s), the acoustoelectric amplification is more pronounced Ge; thus, requires lower electric field to achieve sufficient drift velocity ($v_d = \mu_n E_{dc}$). Figure 1(b) shows the amplification factor (i.e. -α) as a function of E_{dc} applied across a 2×200 μm^2 cross section of (100) Ge waveguide operating at A_0 and S_0 Lamb wave modes. The maximum acoustoelectric amplification occurs for a DC electric field of ~44 V/mm and ~46 V/mm for A_0 and S_0 Lamb waves, respectively.

ALN-ON-GE LAMB WAVE DELAY LINE

To demonstrate acoustoelectric amplification, unidirectional excitation of acoustic wave is instrumental in assuring traveling nature of the propagating wave. In this report, the traveling Lamb waves are excited using a 200 nm AlN piezoelectric film with single phase unidirectional transducers (SPUDT) that ensure excitation/reception of

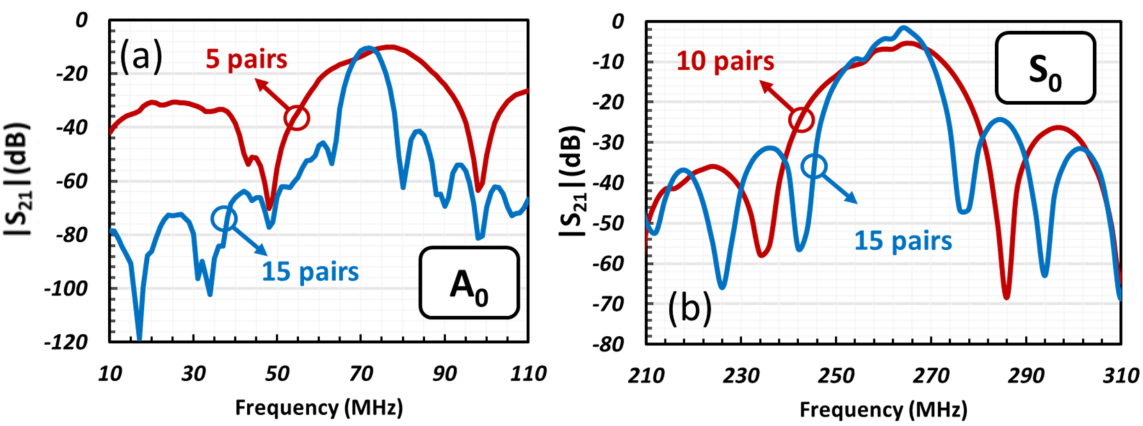

Figure 3: COMSOL-simulated transmission response (i.e. $|S_{21}|$) of the 800μm-long delay line with different SPUDT cell numbers for (a) A_0 and (b) S_0 Lamb waves. The sinc-shaped transfer function for the A_0 and S_0 modes are located at 70 MHz (for 5 and 15 pairs of SPUDT cells) and 261 MHz (for 10 and 15 pairs of SPUDT cells), respectively. The slanted / non-symmetric pass-band of the S_0 delay line is attributed to the phase velocity dispersion. In the simulations, perfectly matched mechanical boundaries, at the two terminations of delay lines, along with matched-impedance electrical termination are used.

traveling wave in forward direction only while suppression of backward reflections [8]. Figure 2(b) shows the SPUDT cell design which has been used to generate acoustic wave in AlN-on-Ge delay lines and corresponding spectral analysis of SPUDTs using delta model [9]. The FEM simulated forward transmission response ($|S_{21}|$) is shown in Figure 3 for A_0 and S_0 modes with different SPUDT cells, assuming material to be lossless and RF terminations matched.

DEVICE FABRICATION

The AlN-on-Ge delay lines are fabricated using a five (5) mask process. The fabrication process flow is depicted in Figure 4. A 2μm thick epitaxial Ge is grown on a sacrificial silicon dioxide (SiO_2)-on-Silicon (Si) substrate. A 20 nm seed AlN layer is sputtered prior to trasnducer stack Mo (50 nm)/AlN (200 nm)/Mo (50 nm) deposition. The seed layer serves as an electrical isolation between RF signals applied to transducers from the DC electric field in Ge. Then SPUDTs are patterned in top Mo along with RF signal pads, and access windows are opened for RF grounds. Furthermore, piezoelectric stack and seed AlN is patterned for DC biasing across Ge waveguide. Next, trenches are etched to define lateral geometry of the delay line. Finally, device is released using holes from top by etching sacrificial SiO_2 in hydrofluoric acid (HF). Figure 5 shows the cross sectional SEM of the stack before release. Figure 6 shows the SEM images of the fabricated AlN-on-Ge Lamb wave delay lines.

EXPERIMENTAL RESULTS

The spectral response of the fabricated delay lines is measured using Keysight N5222A Vector Network Analyzer (VNA). The electrical signals are excited/sensed at the two ports using HL 9402 RF Baluns to enhance the electromechanical coupling. The DC electric field is applied along the Ge waveguide using a Keysight E36105A power supply.

Figure 7(a) and 7(b) manifests the measured transmission responses of the delay line in A_0 (at 70 MHz) and S_0 (at 225 MHz) modes, for different applied DC electric field. Large acoustoelectric amplifications of ~6 dB

Figure 4: Fabrication process flow of for implementation of AlN-on-Ge delay lines. Top Mo SPUDTs serve as RF signal pads and bottom Mo serve as GND pad. The DC bias is applied by accessing Ge. The DC and RF fields are isolated through a 20nm AlN layer.

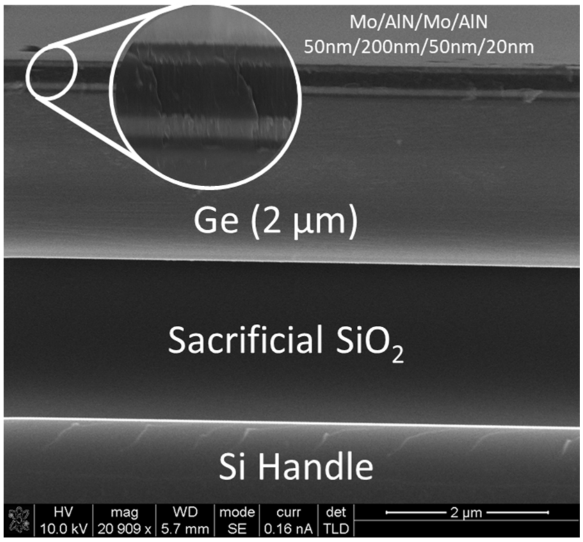

Figure 5: Cross-sectional SEM image of the fabricated AlN-on-Ge delay line: stack of Mo/AlN/Mo/AlN-seed/Ge/Si-seed/Sacrificial SiO_2/Si Handle. The inset shows the details of the piezoelectric transducer stack.

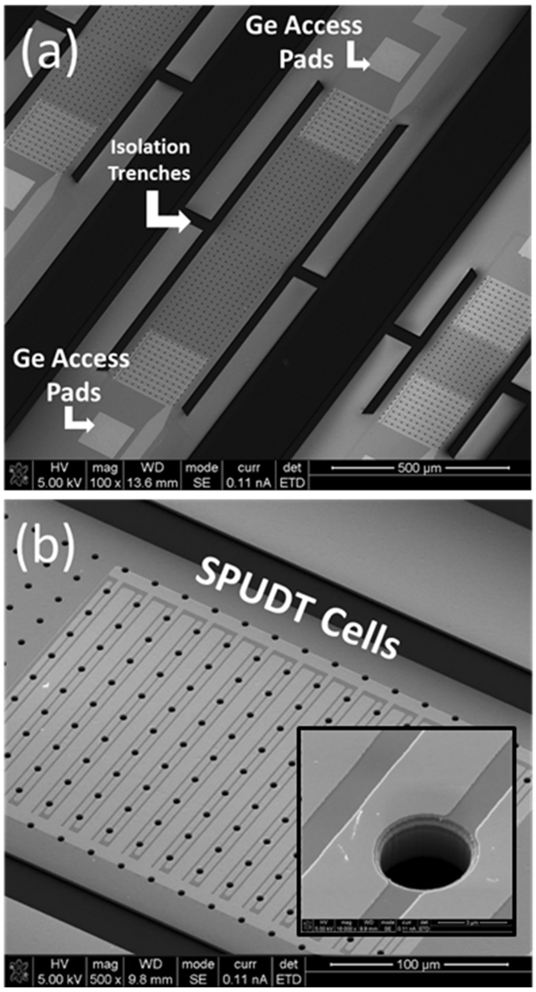

Figure 6: The SEM images of the delay line highlighting (a) the lateral geometry of defined by isolation trenches, the input / output SPUDT ports, and the Ge access pads to apply acoustoelectric DC bias across the waveguide; (b) the zoomed-in image of SPUDT port composed of 15 cells. The inset shows zoomed-in image of a hole etched through the stack to enable release of the delay line by etching sacrificial SiO_2 in HF.

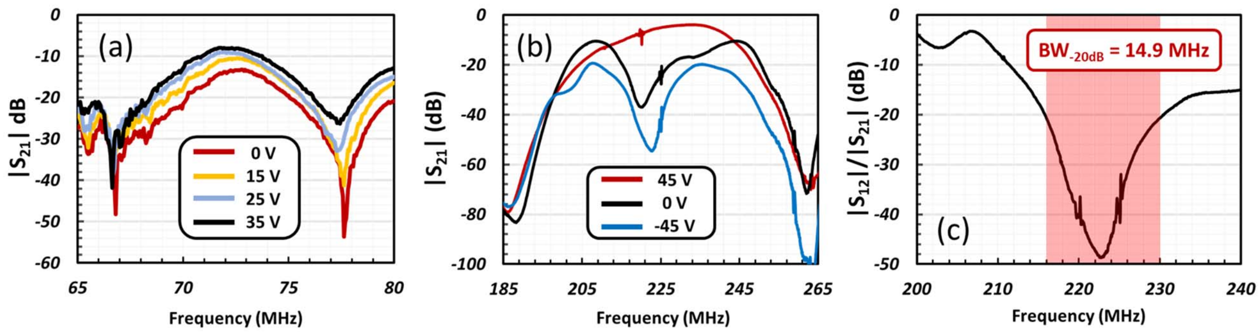

Figure 7: The measured transmission response (i.e. $|S_{21}|$) of the 800µm-long AlN-on-Ge delay line, with 15 SPUDT cells, for different acoustoelectric DC bias voltages when operating in (a) A_0 mode and (b) S_0 mode. Amplification levels of ~6 dB (with 35V of DC bias) and ~7 dB (with 45V of DC bias) are measured for A_0 and S_0 modes, respectively. (c) The measured non-reciprocal transmission ratio (i.e. NTR = $|S_{21}|/|S_{12}|$) for the S0 mode, when a 45V DC bias is applied across the Ge waveguide. While the wave is amplified in the forward direction (corresponding to S_{21}), it gets attenuated in reverse direction (corresponding to S_{12}). A 14.9 MHz of >20dB NTR corresponds to a fraction bandwidth of 6.7%.

and ~ 7 dB are achieved for A_0 and S_0 modes through the application of 35 V and 45 V respectively. Figure 7(c) shows the non-reciprocal transmission ratio (i.e. NTR = $|S_{12}|/|S_{21}|$) for the delay line operating in the S_0 mode, when 45 V acoustoelectric DC bias voltage is applied. While the DC bias amplifies acoustic wave in forward direction, it induces excessive attenuation in reverse direction. A large NTR of ~20 dB is achieved over a 14.9 MHz bandwidth, which corresponds to 6.7 % of the center frequency.

CONCLUSION

This paper reports, for the first time, on the use of acoustoelectric amplification in single crystal Ge for realization of non-reciprocal RF delay lines. This amplification is enabled by the deformation potential scattering physics that couple acoustic waves to electronic band structures in Ge. Analytical formulation is presented showing the large amplification factors for A0 and S0 Lamb waves, when a sufficiently large DC polarization field is applied in the propagation direction. AlN-on-Ge delay line prototypes are designed and implemented operating at 72 MHz and 225 MHz, showing an amplification of ~6 dB and ~7 dB with the application of 35V and 45V DC voltages, respectively. A non-reciprocal transmission ratio in excess of ~20 dB is measured for the S0 wave over a 14.9 MHz bandwidth (i.e. 6.7% of the center frequency), highlighting the potential of Ge-based delay lines for realization of non-reciprocal spectral processors to enable integrated full-duplex RF front-end modules.

ACKNOWLEDGEMENT

We would like to thank staffs in Nanoscale Research Facility (NRF), University of Florida for their valuable suggestion in completing the work. We would also like to thank members of Phononic Sensors and Actuators Lab (PSAL) members for their support. This work is supported by the NSF grant ECCS 1752206.

REFERENCES

[1] Estep, N.A., Sounas, D.L. and Alù, A, "Magnetless microwave circulators based on spatiotemporally modulated rings of coupled resonators", *IEEE TMTT*, vol. 64 (2), pp.502-518, 2016.

[2] Reiskarimian, N. and Krishnaswamy, H., "Magnetic-free non-reciprocity based on staggered commutation", *Nat. Comm.*, vol. 7, p 112117, 2016.

[3] Ghatge, M., Walters, G., Nishida, T. and Tabrizian, R., "A non-reciprocal filter using asymmetrically transduced micro-acoustic resonators", *IEEE EDL*, vol. 40 (5), pp. 800-803, 2019.

[4] Zhu, H. and Rais-Zadeh, M., "Non-reciprocal acoustic transmission in a GaN delay line using the acoustoelectric effect", *IEEE EDL,* vol. 38(6), pp.802-805, 2017.

[5] M. Rotter, A. Wixforth, W. Ruile, D. Bernklau, and H. Riechert, "Giant acoustoelectric effect in GaAs/LiNbO3 hybrids," *Appl. Phys. Lett.*, vol. 73, pp. 2128-2130, 1998.

[6] Bhaskar, U.K., Bhave, S.A. and Weinstein, D., "Silicon acoustoelectronics with thin film lithium niobite", *J. of Phys. D: Appl. Phys.*, vol. 52(5), p.05LT01, 2018.

[7] M. Pomerantz, "Ultrasonic loss and gain mechanisms in semiconductors", *Proc. IEEE*, vol. 53, pp. 1438-1451, 1965.

[8] Lu R, Yang Y, Li MH, Manzaneque T, Gong S., "GHz Broadband SH0 Mode Lithium Niobate Acoustic Delay Lines", *IEEE TUFFC*. Vol. 66 (8), pp-1373-1386, 2019.

[9] Colin Campbell, *Surface Acoustic Wave Devices and Their Signal Processing Applications*, Academic Press, San Diego, CA, USA, 1989.

CONTACT

*Faysal Hakim, tel: +1=352-7459511; hakimfaysal@ufl.edu